Gyrophase-restricted 100 keV–2 MeV ion beams near the foreshock boundary

K. Meziane,[1] M. Wilber,[2] R. P. Lin,[2,3] and G. K. Parks[2]

Received 23 April 2003; revised 25 August 2003; accepted 12 September 2003; published 24 October 2003.

[1] We report on gyrophase-restricted ion beams with energies extending from ~100 keV up to ~2 MeV, observed by Wind in the Earth's distant (~65 R_E) foreshock. The ion gyrophases seen were nearly constant during periods when the distance to the shock contact point could be expected to vary by several R_E, when there was no significant wave activity. At times the distributions had two peaks ~180° apart in gyrophase. These were consistent with a remotely-sensed energetic ion foreshock region having a thickness <2 gyroradii (~1.5 R_E for 0.5 MeV protons with pitch-angle α = 30°). In this picture, gaps in phase space would correspond to particles with guiding centers outside of the energetic foreshock region. Similar observations over a decade of energies (100 keV–2 MeV) suggest that the region thickness scales with gyroradius. According to this interpretation, we have determined a rough range of geometries for which energetic particle production is favored. (Eg., θ_{Bn} ~70–80° for 500 keV ions with α = 30°.) *INDEX TERMS:* 2114 Interplanetary Physics: Energetic particles, heliospheric (7514); 2154 Interplanetary Physics: Planetary bow shocks; 2784 Magnetospheric Physics: Solar wind/magnetosphere interactions; 7807 Space Plasma Physics: Charged particle motion and acceleration; 7851 Space Plasma Physics: Shock waves. **Citation:** Meziane, K., M. Wilber, R. P. Lin, and G. K. Parks, Gyrophase-restricted 100 keV–2 MeV ion beams near the foreshock boundary, *Geophys. Res. Lett.*, *30*(20), 2049, doi:10.1029/2003GL017592, 2003.

1. Introduction

[2] During the past two decades, low-energy (1–10 keV) gyrophase-bunched ions observed upstream of the Earth's bow shock have been studied extensively [*Fuselier et al.*, 1986; *Fazakerley et al.*, 1995; *Meziane et al.*, 2001]. It is now understood that these distributions are produced either through the kinematics of the reflection process [*Gosling et al.*, 1982; *Gurgiolo et al.*, 1983], or through wave-trapping, where the waves are produced by a beam-plasma instability resulting from ions traveling near the upstream limit of the ion foreshock [*Hoshino and Terasawa*, 1985; *Mazelle et al.*, 2003]. From ISEE 1 and 2 timings of >16 keV electrons [*Anderson et al.*, 1979], and asymmetries in 2-D pitch-angle distributions of <40 keV ions and ≲20 keV electrons, *Anderson* [1981] concluded that energetic ions and electrons emanating from the bow shock persist in thin sheets, which for ions may be as small as a few times 10^4 km thick.

[3] Recently, *Meziane et al.* [1999] discussed observations of very-high energy ions (up to ~2 MeV) near the foreshock boundary (θ_{Bn} ~90°, where θ_{Bn} is the angle between the magnetic field and the local shock normal) at distances up to ~60 R_E. These were seen during enhanced fluxes of ambient energetic (E >30 keV) ions, such as those associated with corotating interaction regions (CIRs). A preliminary anlysis of 3-D distributions showed that the ion beams were restricted in gyrophase. However, ultra-low frequency (ULF) wave power sufficient for trapping ~1 MeV ions has never been observed near the foreshock boundary; also, the measured spread in parallel velocity would result in a complete mixing of gyrophases by the time the particles reached the distant observation point [*Gurgiolo et al.*, 1983].

[4] Here we present an analysis of 3-D angular distributions of gyrophase-restricted ions from 100 keV to ~2 MeV, observed ~65 R_E upstream from the bow shock. The sequence and structure of observations indicate that Wind remotely sensed a reflected energetic ion population, whose guiding centers were within a layer of thickness ≲2ρ_i (ρ_i is an ion gyroradius). Such a detailed examination of these distributions is important for understanding the mechanisms leading to the acceleration and reflection of energetic particles at the bow shock and their propagation away from it.

2. Observations

[5] Energetic particle measurements were obtained by the 3-D Plasma and Energetic Particles (3DP) experiment [*Lin et al.*, 1995] on Wind. Three pairs of double-ended solid state telescopes (SSTs), each with either a pair or triplet of closely-stacked silicon semiconductor detectors, provide a full 4\π sr coverage with 36° × 22.5° angular resolution for electrons >20 keV and ions >30 keV. One side of the detector stack has a thin lexan foil, chosen to stop protons up to ~400 keV while leaving electrons virtually unaffected. The opposite end is open, but has a magnet that sweeps away electrons below ~400 keV while leaving ions unaffected. Thus, in the absence of higher-energy particles, ions and electrons are cleanly separated. When higher-energy ions are present (up to 6 MeV stop in the detector), they are counted by the Open SST and their contribution to the Foil SST can be computed. More massive ions require higher energies to penetrate the foil, and by comparing the responses of the Open and Foil SSTs some composition information can be obtained. The field data are from the Magnetic Field Investigation [*Lepping et al.*, 1995].

[6] Figure 1 shows observations from 1645–1700 UT on 6 December 1994, while Wind was at (53, −40, −2)R_E (GSE). During this interval the interplanetary medium was

[1]Department of Physics, University of New Brunswick, Fredericton, Canada.
[2]Space Sciences Laboratory, U. California, Berkeley, USA.
[3]Department of Physics, U. California, Berkeley, USA.

0094-8276/03/2003GL017592$05.00

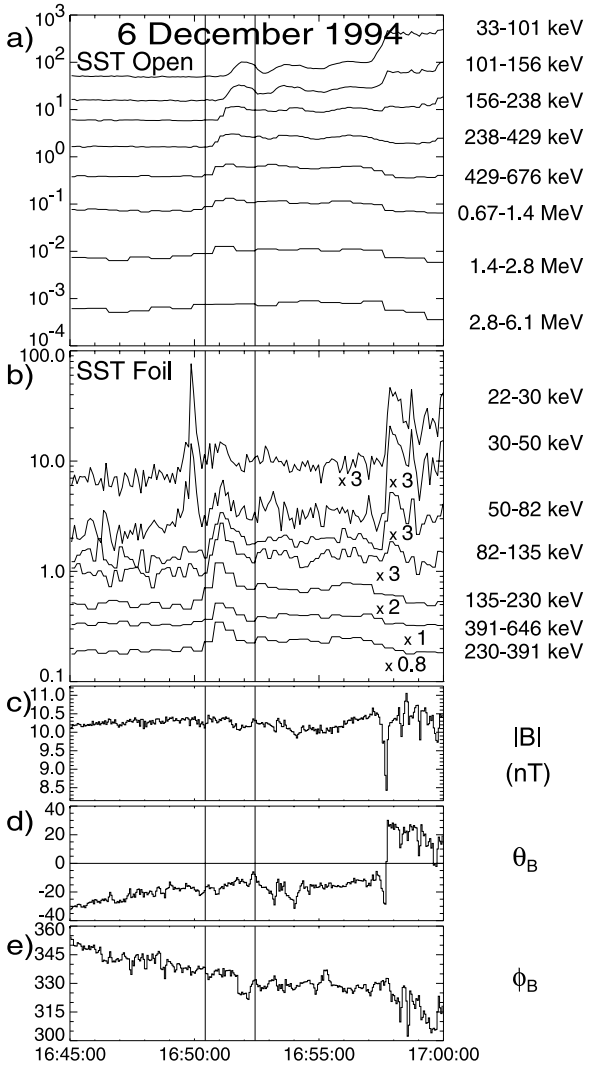

Figure 1. a) Ion fluxes ($s^{-1}cm^{-2}keV^{-1}$) from the Open SST; b) fluxes from the Foil SST (primarily electrons); magnetic field c) magnitude B, d) polar angle θ_B, and e) azimuthal angle in ϕ_B GSE coordinates. The two vertical lines delimit the interval shown in Figure 2.

bathed in high fluxes of energetic (30 keV–6 MeV) particles associated with the passage of a CIR.

[7] Wind crossed the electron foreshock boundary at 1649:56 UT, as indicated by the 22–50 keV spikes in the Foil SST fluxes. This was corroborated by an intense burst of electrostatic wave power, especially near the electron plasma frequency, detected by the WAVES-TNR experiment [*Bougeret et al.*, 1995] (data not shown). Shortly afterwards the Open SST detected a dispersive burst of ions starting prior to 1650:38 UT, with the lower-energy particles arriving at the spacecraft after those having higher energies. The dispersion is not resolved by the SST above 429–676 keV. The coincident counts in the Foil SST at all energies during this interval are due to protons that have penetrated the lexan. (Higher mass ions would not penetrate the foil with the fluxes observed in the highest energy channels.)

[8] The magnetic field magnitude (Figure 1c) was steady at ~10.5 nT until 1657:30 UT, showing no indication of compressional waves. Aside from ±2° fluctuations, θ_B (Figure 1d) showed a quasi-monotonic change from −30° to −10°, and ϕ_B (Figure 1e) steadily declined through 1652:20 UT as the field slowly rotated dawnward. Assuming a paraboloidal shock matching the observed upstream conditions, $x = a_s - b_s (y^2 + z^2)$, with $a_s = 11.8\ R_E$ and $b_s = 0.026\ R_E^{-1}$, [*Cairns et al.*, 1995], the decline in the polar angle in particular is consistent with the observed connection to the shock starting at 1649:56 UT. At 1652:20 UT the interplanetary magnetic field (IMF) rotated more than 20° towards south, while the azimuthal angle leveled-off.

[9] Figure 2 presents 2-D particle distributions in gyrophase and pitch-angle for three Open SST energies, after subtraction of the CIR background population (bottom row), obtained near 16:48 UT, prior to Wind's connection to the shock. The top panel of the left column shows the initial detection of sunward-streaming 429–676 keV protons. The peak is not aligned with the magnetic field, but instead is centered at $\alpha \sim 30°$, and is constrained to a narrow range of gyrophases. 24 seconds later the distribution shows a strong maximum in phase space density (PSD) near the same gyrophase and pitch angle as the original, with intermediate strength (green) PSDs forming a nearly-complete ring. Subsequent observations show a broadening of the more-intense regions on the left half of the distributions, and some brightening on the right. By 1652:02–1652:26 UT the distribution has reverted to having a 'one-sided' form for the most intense phase space densities. The intermediate PSDs continue to form a nearly-complete ring.

[10] The middle column shows 238–429 keV particles at twice the time resolution of the 429–676 keV channel, and these exhibit similar behavior. The differences are that the initial onset occurs ~12 s later, and the return to a dominantly one-sided distribution occurs some 48 s earlier than for the more-energetic protons. The 156–238 keV ions (right hand column) also show trends similar to the 429–676 keV ions. These first appear an additional ~12 s later than the 238–429 keV particles, but persist with a 'two-sided' form until 1651:38 UT, which is intermediate between the times when this transition occurred for the other two channels. The return to one-sided distributions is roughly coincident with the onset of the rotation in θ_B at 1652:20 UT.

[11] The spread in gyrophase appears not to be affected by the integration time of the detector. The 33–101 keV and 101–156 keV channels (not shown) have 6 s (2 spin) integrations, roughly equal to a proton gyroperiod. These exhibit similar gyrophase limits as seen in the higher-energy channels, which integrate for 12 s and 24 s. It is also noteworthy that the gyrophases of the more-intense fluxes remain relatively stable over much of the 1 $\frac{1}{2}$-minute interval.

3. Discussion

[12] The observed gyrophase-restricted distribution functions of Figure 2 cannot be explained solely on the basis of production mechanisms at the shock, or active trapping by a local wave field. If the kinematics of particle reflection at the shock were to cause them to emerge at narrowly-defined gyrophases, these particles could be expected to mix completely in phase well before reaching Wind at distances >50 R_E from the shock, as the result of the spread in their observed parallel velocities. In particular, for the $\alpha \sim 30°$ distributions observed here, the $\Delta E/E \sim 0.25$ passband of the SSTs and an estimated $\Delta\alpha \sim 20°$, protons would be

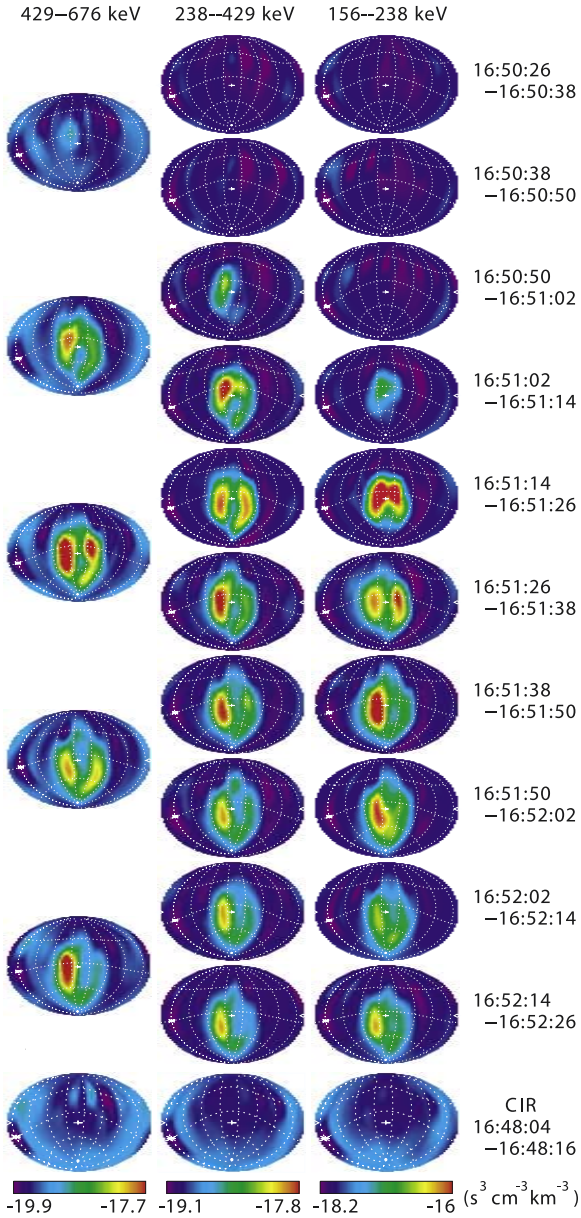

Figure 2. 2-D PSDs from the Open SST (solar wind frame) for energies (a) 429–676 keV, (b) 238–429 keV, and (c) 156–238 keV. Hammer-Aitoff projections display a full 4 π sr, and the 3 channels together present a portion of the measured 3-D phase space. **B** points out of the page at the center of each panel, and an asterisk indicates the solar wind direction. CIR populations (bottom row) have been subtracted.

fully gyrophase-mixed by the time they crossed upstream distances of 17 R_E, 20 R_E and 28 R_E, respectively, for energies of 156–238 keV, 238–429 keV and 429–676 keV. In addition, we know of no production mechanism that predicts two-sided PSDs (peaks 180° apart in gyrophase).

[13] We estimated shock distances by tracing observed fluxes back to a model shock (described above) and found changes during 16:51–16:52 UT corresponding to several gyro-orbits of travel for the observed energies and pitch angles. However, there was relatively little change in the observed gyrophases of the peak fluxes, contrary to expectations for travel along 'standing' gyrating particle structures. We do not expect particle trapping to work in this case because this would require high amplitude, nearly-monochromatic waves.

[14] A possible explanation for these observations comes from noting the large ~1 R_E gyroradii of these particles. Figure 3a depicts the overall geometry (here rotated about x_{GSE} so that south is up, for clarity). The green and blue surfaces represent the limits of the energetic ion foreshock, as defined by the orbit guiding centers. The red curve shows the trajectory of a particle centered just interior to the layer, that could be among the first detected when the spacecraft is $\lesssim 1\rho_i$ of the blue surface. Figures 3b and 3c shows particle orbits (as would be computed in the solar wind frame) projected onto the plane normal to **B** and centered on Wind. The dimensions (units of R_E) correspond to 500 keV protons with $\alpha = 30°$. Grey shading represents the cross section of the energetic ion foreshock. Initially, Wind will remotely sense particles whose guiding centers are on the locus of points (dotted black) interior to the layer and within $1\rho_i$ of the spacecraft (Figure 3b). The gyrophase extent of the particles detected (represented as green arcs) will extend past 180° as Wind enters the layer, and can span a full 360° (forming a ring in this plane) when the spacecraft is $1\rho_i$ interior to its edge. However, if the layer thickness is $<2\ \rho_i$, a gap in the observable phase space will open up before the ring has closed, leaving two opposing arcs (Figure 3c).

[15] In this scenario, particles gyrating about a given guiding center would be fully mixed in gyrophase by the

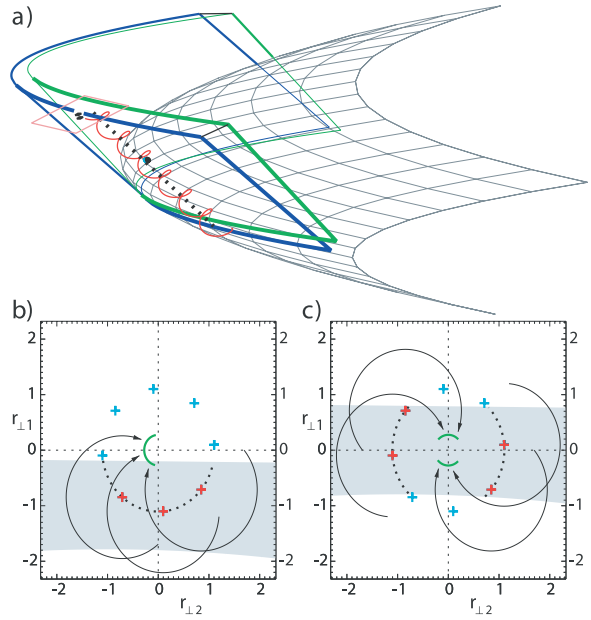

Figure 3. a) Cartoon of thin layer geometry. Grey mesh is shock surface, and blue (green) surfaces delimit sunward (anti-sunward) extents of energetic ion guiding centers. a representative particle orbit (red) has its guiding center just interior to the layer; b) and c) sketch physical space source of observed particles in a thin sheet model. Black arcs are projections of particle trajectories onto the **B**-normal plane, and red '+'s are corresponding guiding centers. Guiding centers inside the layer (red correspond to observed fluxes (represented as small green arcs in the center), and light blue '+'s indicate guiding centers outside the sheet (no fluxes).

time they reached Wind. The relatively steady phases seen would result in spite of large changes in the distance to the shock, provided that the orientation of the layer remained fairly steady, since the layer edges determine the limits of the observed phases. The observations explicitly require of this explanation that the thickness of the layer scales with gyroradius, as the higher-energy detector channels see approximately the same portions of gyrophase depleted of fluxes as do the lower-energy channels. We note that the several $\times 10^4$ km ion foreshock thickness inferred by *Anderson* [1981] using modeled times of flight for various energies and pitch angles is roughly an order of magnitude larger than our result of $\lesssim 1\ R_E$ for $\sim$100 keV protons. We note that the layer thickness can also be equated to a range of θ_{Bn} values where particles from the inner and outer edges trace back to the bow shock. Using the model bow shock described above and guiding center paths, we found good agreement with the observations for 500 keV, $\alpha = 30°$ ions by setting bounds on the source region such that $70 \lesssim \theta_{Bn} \lesssim 80°$. This range would scale with particle gyroradius.

[16] If we consider the source of the ions forming these thin layers, the possibilities include: 1) energetic ions escaping from the magnetosheath, or upstream particles that are energized through 2) Fermi acceleration, or 3) the shock drift mechanism. A magnetosheath source is unlikely, given the peak in fluxes at $\alpha \gtrsim 30°$ and the quasi-perpendicular shock geometry. Escape would be favored for particles with most of their momentum directed upstream (small αs), and the field reduction in crossing the bow shock would tend to decrease their pitch angles further. (To have a peak at $\alpha = 30°$ after travelling through the shock, assuming approximate μ-conservation, the source magnetosheath distribution would need to be peaked at $\gtrsim 60°$, but we have no a priori basis for expecting this.) Fermi acceleration is unlikely because of the lack of observed upstream waves needed to scatter or reflect the ions back to the shock, and because the bursts were observed shortly after the electron foreshock.

[17] In contrast, all observations are consistent with the shock drift acceleration (SDA) mechanism, which favors pitch angles determined by the mirror ratio at the point of reflection in the shock ($\alpha = \sin^{-1}(B_o/B_r)^{\frac{1}{2}}$), for B_o the field strength at the observation point in the solar wind and B_r the field strength at the reflection point). SDA also favors θ_{Bn} approaching 90°, and the high energies observed. The observed spectrum in this case has been well modeled by calculations (not shown) assuming single-event adiabatic mirroring in the de Hoffman-Teller frame of reference [*deHoffman and Teller*, 1950], given the observed enhanced energetic background spectrum. *Meziane et al.* [1999] presented such a comparison for an event observed earlier on this day within the same CIR. In the picture we present here, forward dispersion (not expected for Fermi acceleration) results from the remote sensing of larger gyroradius particles first. In this and most of the several comparable cases reviewed to date, there is evidence of an energized solar wind component that could serve as a seed population. However, preliminary analysis has uncovered examples of similar very energetic upstream ions when no energetic solar wind component is present. This is a topic for further study.

[18] If, as we assert here, we have determined the width of the energetic ion foreshock, we have also determined the size of the region on the shock itself for which energetic ion production is favored; namely, $d \lesssim 2\ \rho_i/\sin\theta_{Bn}$. (This differs from the much broader scales typical of $\lesssim$20 keV beams, and still wider regions found for intermediate and diffuse populations.) This relation, appearing here to scale with gyroradius, places an important, testable constraint on models used to explain the reflection, and will be the focus of future work.

[19] **Acknowledgments.** We thank R. P. Lepping for providing the MFI data. Work at U.N.B. was funded by grants from the Canadian Natural Science and Engineering Research Council, and at U.C.B. by NASA grant NAG5-11804.

References

Anderson, K. A., Measurements of bow shock particles far upstream from the Earth, *J. Geophys. Res.*, *86*, 4445–4454, 1981.

Anderson, K. A., R. P. Lin, F. Martel, C. S. Lin, G. K. Parks, and H. Rème, Thin sheets of electrons upstream from the Earth's bow shock, *Geophys. Res. Lett.*, *6*, 401–404, 1979.

Bougeret, J.-L., et al., WAVES: The radio and plasma wave investigation on the WIND spacecraft, *Space Sci. Rev.*, *71*, 231–263, 1995.

Cairns, I. H., D. H. Fairfield, R. R. Anderson, V. E. H. Carlton, K. I. Paularena, and A. J. Lazarus, Unusual locations of Earth's bow shock on September 24–25, 1987: Mach number effects, *J. Geophys. Res.*, *100*, 47–62, 1995.

deHoffman, F., and E. Teller, Magneto-hydrodynamic shocks, *Phys. Rev.*, *80*, 692–703, 1950.

Fazakerley, A. N., A. J. Coates, and M. W. Dunlop, Observations of upstream ions, solar wind ions and electromagnetic waves in the Earth's foreshock, *Advances in Space Research*, *15*, 103–106, 1995.

Fuselier, S. A., M. F. Thomsen, J. T. Gosling, S. J. Bame, and C. T. Russell, Gyrating and intermediate ion distributions upstream from the Earth's bow shock, *J. Geophys. Res.*, *91*, 91, 1986.

Gosling, J. T., M. F. Thomsen, S. J. Bame, W. C. Feldman, G. Paschmann, and N. Sckopke, Evidence for speculary reflected ions upstream from the quasi-parallel bow shock, *Geophys. Res. Lett.*, *87*, 1333–1336, 1982.

Gurgiolo, C., G. K. Parks, and B. H. Mauk, Upstream gyrophase bunched ions: A mechanism for creation at bow shock and the growth of velocity space structure through gyrophase mixing, *J. Geophys. Res.*, *88*, 9093–9100, 1983.

Hoshino, M., and T. Terasawa, Numerical study of the upstream waves excitation mechanism, 1, nonlinear phase bunching of beam ions, *J. Geophys. Res.*, *90*, 57–64, 1985.

Lepping, R. P., et al., The Wind magnetic field investigation, *Space Sci. Rev.*, *71*, 207–229, 1995.

Lin, R. P., et al., A three-dimensional plasma and energtic particles investigation for the Wind spacecraft, *Space Sci. Rev.*, *71*, 125–206, 1995.

Mazelle, C., et al., Production of gyrating ions from nonlinear wave-particle interaction upstream from the Earth's bow shock: A case study from Cluster-CIS, *Planet. Space Sci.*, in press, 2003.

Meziane, K., R. P. Lin, G. K. Parks, D. E. Larson, S. D. Bale, G. M. Mason, J. R. Dwyer, and R. P. Lepping, Evidence for acceleration of ions to $\sim$1 MeV by adiabatic-like reflection at the quasi-perpendicular Earth's bow shock, *Geophys. Res. Lett.*, *26*, 2925–2928, 1999.

Meziane, K., C. Mazelle, R. P. Lin, D. LeQuéau, D. E. Larson, G. K. Parks, and R. P. Lepping, Three-dimensional observations of gyrating ion distributions far upstream from the Earth's bow shock and their associated with low-frequency waves, *J. Geophys. Res.*, *106*, 5731–5742, 2001.

K. Meziane, Physics Department, University of New Brunswick, P.O. Box 4400, Fredericton, NB, E3B 5A3 Canada. (karim@unb.ca)

M. Wilber, R. P. Lin, and G. K. Parks, Space Sciences Laboratory, U. California, Berkeley, CA 94720, USA.